Available online at www.sciencedirect.com
SCIENCE DIRECT
Polymer 47 (2006) 3568–3575
polymer
www.elsevier.com/locate/polymer

Creep and recovery behaviors of a polythiophene-based electrorheological fluid

Datchanee Chotpattananont [a], Anuvat Sirivat [a,*], Alexander M. Jamieson [b]

[a] *Conductive and Electroactive Polymers Research Unit, The Petroleum and Petrochemical College, Chulalongkorn University, Soi Chula 12, Phyathai Road., Bangkok 10330, Thailand*
[b] *Department of Macromolecular Science, Case Western Reserve University, Cleveland, OH 44106-7202, USA*

Received 28 July 2005; received in revised form 18 January 2006; accepted 18 March 2006

Abstract

We investigate the creep response of poly(3-thiopheneacetic acid) (PTAA) particles doped with perchloric acid. With increase in applied stress, these suspensions exhibit an evolution from a linear viscoelastic response, with three components of instantaneous elastic strain, retarded elastic strain and viscous strain, to a nonlinear viscoelastic response, where the retarded elastic and viscous strains monotonically decrease and a plastic contribution to the instantaneous strain grows, followed by a viscoplastic solid behavior, with fully plastic instantaneous strain, and finally a transition from plastic solid to a plastic liquid at the yield stress. With increase in electric field strength at fixed particle concentration and applied stress, the viscoplastic response diminishes, and more elastic behavior ensues. For highly doped samples, at high-electric field strengths, a fully elastic solid response is observed in the linear viscoelastic regime. The equilibrium compliance, J_C and steady state recoverable compliance J_R, were investigated as a function of electric field strength, particle concentration and particle conductivity. The results are interpreted in terms of the field-induced formation of thick fibrillar aggregates spanning the gap between the electrodes, each consisting of bundles of particle strings. Strings, which are fully connected to both electrodes generate an elastic response to the applied stress, whereas strings which are attached at only one end or are unattached generate a viscoplastic response. The net effect of an increase of the electric field strength, particle concentration, or particle conductivity is an increase in elasticity, i.e. predominantly creation of fully connected particle strings.

Keywords: Conjugated polymer; Creep; Electrorheology

1. Introduction

Electrorheological (ER) fluids composed of polarizable colloidal particles dispersed in a non-conducting fluid have attracted considerable recently [1,2] because many applications based on ER technology are possible, including the active elements of clutches, breaks, shock absorbers, engine mounts, valves, and flow pumps [3–5]. Upon the application of an electric field, chain-like or fibrillar aggregates of the suspended particles are oriented along the direction of the electric field, thereby inducing viscoelasticity and a drastic increase in viscosity [1,2]. Such ER fluids have typically used hydrated organic or inorganic particulates, in which the polarisability arises from ion motion in adsorbed water. More recently, ER fluids have been developed based on semi-conducting polymers, in which the polarisability is due to motion of electrons within the suspended particles. Examples include polyaniline (PANI) and its derivatives [6–10], polypyrrole [11,12], and poly(*p*-phenylene) [13]. Extensive studies have been carried out on the rheological properties of the ER fluids under steady shear and oscillatory shear flows [1,2,6–13], and have established that the suspensions in the presence of an electric field exhibit a yield stress, which increases with particle concentration and field strength, and above which the suspension exhibits viscous flow. In the pre-yield region, a predominantly elastic response to deformation is observed, and, at small strains, a linear viscoelastic description can be adopted. In the post yield region, plastic flow occurs.

Relatively little attention has been paid to the deformational (creep) response, which can provide insight into the mechanistic origin of the flow of ER fluids. Otsubo and Edamura [14] demonstrated that the creep behavior of an ER fluid consisting of TiO_2/polymer composite particles in silicone oil, appears to exhibit an instantaneous elastic response, followed by a retarded elastic deformation, and then viscous flow. At higher

* Corresponding author. Tel.: +66 2218 4131; fax: +66 2215 4459.
E-mail address: anuvat.s@chula.ac.th (A. Sirivat).

0032-3861/$ - see front matter © 2006 Elsevier Ltd. All rights reserved.
doi:10.1016/j.polymer.2006.03.061

stress, closer to the yield point, unexpectedly, the creep shows an elastic solid response, and at still higher stress, in the yield region, the strain increases with time in a stepwise fashion, suggesting sequential rupture and restoration of the fibrillar structure was taking place. A similar behavior was observed for a magnetorheological fluid by Li et al. [15], who further clarified that the creep behavior exhibits a transition from a linear viscoelastic response at the lowest shear stresses, where the instantaneous stress is completely elastic, i.e. fully recoverable, to a nonlinear viscoelastic response at higher stress, where there is a nonrecoverable plastic contribution to the instantaneous stress, which increases in magnitude with increasing stress. At stresses just below the yield point, the material behaves as a viscoplastic solid, i.e. the instantaneous strain is dominantly plastic in nature, and rapidly approaches an equilibrium value, and there is negligible recovered strain on removal of the stress. Finally, at the yield stress, the strain increases continuously in a stepwise fashion with no detectable elastic recovery, corresponding to a transition from a viscoplastic solid to a plastic fluid. See et al. [16] have confirmed the presence of a retardation strain in an MR fluid and point out that this phenomenon is not predicted by current rheological models of field-responsive fluids. Lau et al. [17] report that the yield stress of a model ER fluid based on silica spheres in a silicon oil is enhanced when subjected to repeated cyclic creep tests in the linear viscoelastic regime.

Recently, we reported rheological studies of an ER fluid based on a new semiconducting candidate ER material, poly(3-thiophene acetic acid) (PTAA), doped with perchloric acid ($HClO_4$) [18,19]. $HClO_4$-doped PTAA/silicone oil suspensions show typical Bingham flow behavior upon application of an electric field. The static yield stress increases with electric field strength, E, and particle volume fraction, ϕ, according to the scaling law, $\tau_y \propto E^{\alpha}\phi^{\gamma}$ [19]. The scaling exponents α and γ approach the values of 2 and 1, respectively, predicted by the polarization model [20,21], at low fields, and when the particle volume fraction and the doping level decrease [19]. The frequency-dependent moduli at different electric field strengths and conductivities, when scaled according to the model of Parathasarathy and Klingenberg [22], approximately collapse into master functions of the dimensionless frequency [18]. In the present study, we investigate the creep and recovery behaviors of this ER fluid. The creep and creep recovery behaviors of $HClO_4$-doped PTAA/silicone oil suspensions are investigated as a function of applied stress level, electric field strength, $HCLO_4$ doping level, and particle concentration.

2. Materials and methods

2.1. Materials

3-Thiopheneacetic acid, 3TAA (AR grade, Fluka) was used as the monomer. Anhydrous ferric chloride, $FeCl_3$ (AR grade, Riedel-de Haen) was used as the oxidant. Chloroform, $CHCl_3$ (AR grade, Lab-Scan) and methanol, CH_3OH (AR grade, Lab-Scan) were dried over CaH_2 for 24 h under the nitrogen atmosphere and then distilled. The perchloric acid dopant, $HClO_4$ (AR grade, AnalaR) was used as received. The dispersing phase was silicone oil (AR grade, Dow corning) with density 0.96 g/cm^3 and kinematic viscosity of 100 cSt, and was vacuum-dried and stored in a desiccator prior to use.

2.2. Preparation of ER fluid and creep measurements

Poly(3-thiopheneacetic acid), PTAA was synthesized by the oxidative-coupling polymerization according to the method of Kim et al. [23]. PTAA particles were doped with perchloric acid at various amounts to vary particle conductivity [24]. The electrorheological, ER, fluids were prepared by dispersing the $HClO_4$ doped PTAA particles in silicone oil (density 0.96 g/cm^3 and kinematic viscosity 100 cSt) with an ultrasonicator for 30 min at 25 °C.

The creep and recovery behaviors were investigated using a stress-controlled rheometer (Carrimed, CR50) with 4 cm diameter parallel plate geometry at 25 ± 0.1 °C. The gap for the geometry used was 0.1 mm for each measurement. A DC voltage was applied during the measurements using a high-voltage power supply (Bertan Associates Inc., Model 215). In our sample conditioning, the suspensions were subjected to a steady state shear at 300 s^{-1}, and then electrified in a quiescent state for 5 min, to ensure the formation of equilibrium fibrillar structure before a measurement was taken. A constant stress was then instantaneously applied, maintained for 180 s, and then suddenly removed. The time dependent strain was measured at various electric field strengths. Each measurement was carried out at a temperature of 25 ± 0.1 °C and repeated at least two or three times.

3. Results and discussion

The effect of stress level, particle concentration, and particle conductivity on the creep and recovery properties of the suspensions were investigated. Particle concentrations investigated were 5, 10, and 20% by weight (corresponding to volume fractions of 0.025, 0.048, and 0.092, respectively) at a specific conductivity of 7.5×10^{-2} S/cm (HPT5, HPT10, and HPT20). To explore the influence of conductivity, the particle concentration was fixed at 20% by weight and the particle conductivity values varied from approximately zero (undoped, designated UPT20), 2.0×10^{-4} S/cm (low doping, designated LPT20), and 7.5×10^{-2} S/cm (high-doping, designated HPT20), respectively (Table 1).

First, a series of creep and recovery experiments were conducted using a sequence of step stresses. Creep is the time-dependent evolution in strain (γ) of a viscoelastic material under constant stress, σ_0, [25]. On the removal of stress, some of the time-dependent deformation may be recoverable. A creep test is, therefore, characterized by two distinct phases: the creep phase and the recovery phase. In the creep phase, a constant stress (σ_0) is applied instantaneously to the sample and maintained at that level for a fixed period. For a viscoelastic material, in general, the time dependence of the strain (γ_C) can

Table 1
Properties and yield stress values of PTAA/silicone oil suspensions

ERFs	Particle concentration (wt%)	Particle conductivity (S/cm)	Yield stress, σ_y (Pa)				
			1 kV/mm	1.5 kV/mm	2 kV/mm	2.5 kV/mm	3 kV/mm
HPT5	5	7.5×10^{-2}	20.1	38.5	60.1	113.8	126.5
HPT10	10	7.5×10^{-2}	43.5	84.4	146.1	184.8	275.8
HPT20	20	7.5×10^{-2}	76.5	115.0	187.3	250.3	340.6
LPT20	20	2.0×10^{-4}	44.3	95.5	167.8	221.0	308.1
UPT20	20	3.2×10^{-7}	38.5	58.5	96.5	200.25	286.0

be expressed in terms of three contributions [15];

$$\gamma_C(t) = \gamma_s + \gamma_d(t) + \gamma_v(t), \quad (1)$$

where γ_s is the instantaneous strain, which, for a linear viscoelastic material, represents a purely elastic response to the applied stress ($\gamma_s=\gamma_e$), $\gamma_d(t)$ is the retardation strain which describes a delayed elastic response, requiring time to develop fully, and $\gamma_v(t)$ is the viscous flow or the irreversible component of strain. For linear viscoelastic materials, the instantaneous strain γ_s and the retardation strain $\gamma_d(t)$ are reversible, and fully recover on removal of the applied stress. However, for nonlinear viscoelastic materials, the instantaneous strain γ_s may consist of an elastic component and a plastic component, ($\gamma_s=\gamma_e+\gamma_p$); γ_p, like the viscous strain $\gamma_v(t)$ cannot be recovered after unloading. Thus, in the recovery phase, for both linear and nonlinear viscoelastic materials, the time dependent recoverable strain $\gamma_R(t)$ consists of an instantaneous component, $\gamma_r=\gamma_e$, and a time-dependent component whose amplitude is γ_d:

$$\gamma_R = \gamma_e + \gamma_d \quad (2)$$

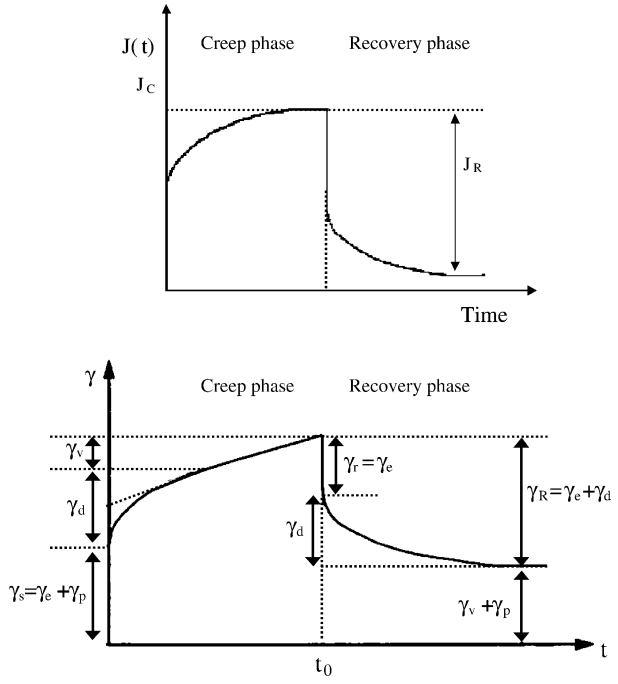

Fig. 1. Schematic diagram of the creep and creep recovery curves under a constant applied shear stress for a nonlinear viscoelastic material.

Fig. 1 shows a schematic of a typical creep test performed on a nonlinear viscoelastic material.

The material property which characterizes the creep behavior is the creep compliance, $J(t)=\gamma(t)/\sigma_0$. For a viscoelastic solid, at long times after the stress is applied, creep is arrested, and one can define the equilibrium creep compliance J_C as the steady state strain, $\gamma_C=\gamma_e+\gamma_p+\gamma_d(\infty)$, divided by the stress, σ_0. Likewise, at long times after the stress has been removed, creep recovery is arrested, and one can define the equilibrium recovery compliance J_R as the total recoverable strain, $\gamma_R=\gamma_e+\gamma_d(\infty)$, divided by the stress, σ_0. [25]. If the sample is a viscoelastic fluid, the strain will continue to increase as long as the stress is applied, and the viscosity can be determined as the inverse of the slope $=\mathrm{d}J(t)/\mathrm{d}\gamma$ in the steady flow region [25].

For ER fluids, it behaves as purely viscous material under no electric field, in which material deforms steadily under stress. The deformation of purely viscous material is the permanent deformation or no recovery take place after the stress is removed. In contrast, the viscoelastic response of the ER fluids can be observed when an electric field is applied. This viscoelastic response of the ER fluids arises from the chain-like or fibrillar aggregates of the suspended particles. The schematic of a creep test performed on an ER fluid with and without the application of electric field is illustrated in Fig. 2.

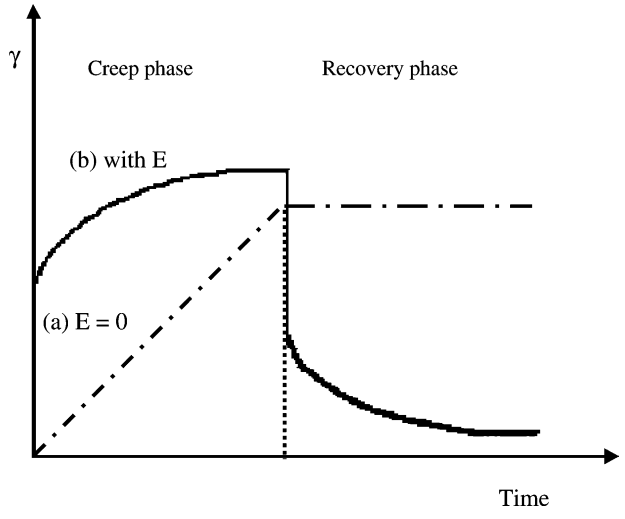

Fig. 2. Schematic diagram of the creep and creep recovery curves under a constant applied shear stress for an ER fluid; (a) without electric field and (b) with electric field.

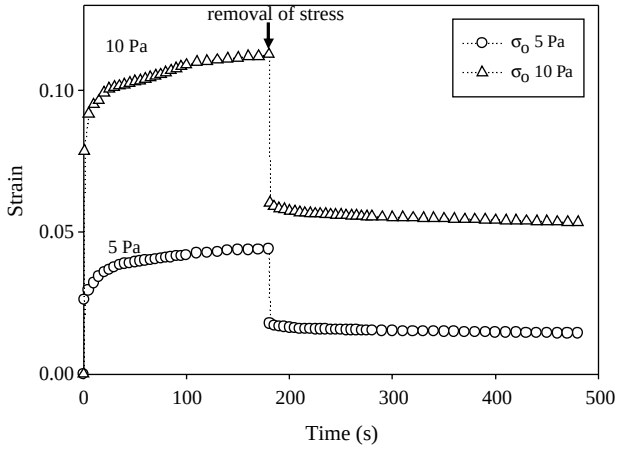

Fig. 3. Creep response of the 20 wt% highly doped PTAA suspension under the electric field strength of 1 kV/mm at various applied stress values: (○) 5 Pa and (△) 10 Pa.

Figs. 3 and 4 show the creep and recovery curves for a 20 wt% highly doped polythiophene suspension (HPT20) under a constant electric field strength of 1 kV/mm. We have recently reported that the yield stress value of the HPT20 suspension at a field strength of 1 kV/mm is 76.5 Pa [19]. The creep tests were conducted below the yield stress regime: applied stresses were varied from 5 to 76.5 Pa.

From Fig. 3, at the stress lowest level, 5 Pa, we see that, consistent with previous studies of ER and MR fluids, the creep curve comprises three parts: the instantaneous strain, the retardation strain, and the viscous strain, viz. γ_s, $\gamma_d(t)$, and $\gamma_v(t)$. Also, the sample shows an instantaneous elastic recovery, γ_r, followed by a slower recovery process when the applied stress is removed. It is apparent that at this stress level, the sample is in the linear viscoelastic regime, as evidenced by the fact that the instantaneous strain equals the instantaneous elastic recovery, i.e. $\gamma_s = \gamma_r = \gamma_e$. At a stress level of 10 Pa, the creep curve still exhibits the three strain components. However, we are now in the nonlinear strain regime, since the instantaneous recovered strain is manifestly smaller than that on the application of stress, i.e. $\gamma_s = \gamma_e + \gamma_p > \gamma_r$.

We expect on the basis of previous studies [14,15] that the plastic strain increases uniformly with further increase of the applied stress up to the yield stress, and this is indeed confirmed as shown in the creep curves at applied stresses of 50 and 70 Pa in Fig. 4. In each case, the instantaneous strain is very large, there is a small retarded strain, and the strain rapidly attains a constant equilibrium value with no viscous strain. It can be deduced from these results that the suspension behaves essentially like a plastic solid, with a completely plastic instantaneous strain, and negligible strain recovery after the removal of stress. When the applied stress is increased to 76.5 Pa, which corresponds precisely to the yield stress (Fig. 4), we see that the strain increases rapidly continuously with time in a stepwise manner. In addition, there is no instantaneous elastic recovery when the applied stress is removed. Thus it appears our ER fluid based on $HCLO_4$-doped PTAA, passes through the sequential regimes of behavior recognized in an ER fluid by Otsubo and Edamura [14], and in an MR fluid by Li et al. [15], viz. linear viscoelasticity, nonlinear viscoelasticity, viscoplastic solid and a transition from plastic solid to plastic liquid.

The plastic response at higher stresses is attributed [14,15] to the existence of thick fibers, which contain particle chains connected at both electrodes, chains attached at only one end, and drifting chains, unattached at both ends. The attached chains are responsible for the elastic response, the unattached chains are responsible for energy dissipation through particle motion. With increasing applied stress, more stress is dissipated giving an increasingly plastic response. At the yield point, the fiber structure repeatedly breaks down and reforms into a new structure, giving the stepwise creep response [14,15].

Fig. 5 shows the % recoverable strain of the 20 wt% HPT20 suspension as a function of applied stress at various electric

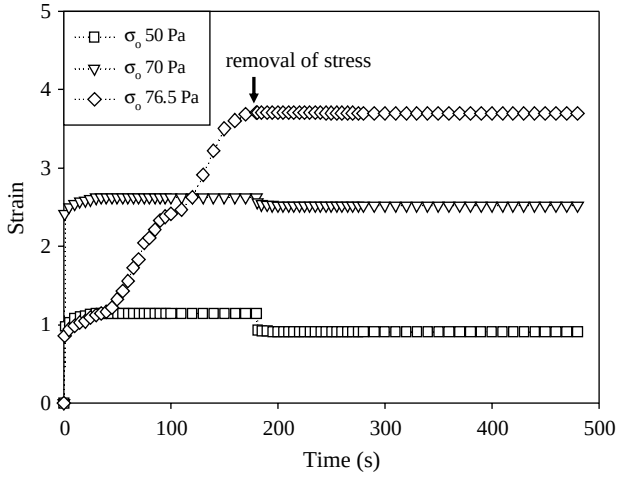

Fig. 4. Creep response of the 20 wt% highly doped PTAA suspension under the electric field strength of 1 kV/mm at various applied stress values: (□) 50 Pa, (▽) 70 Pa, and (◇) 76.5 Pa.

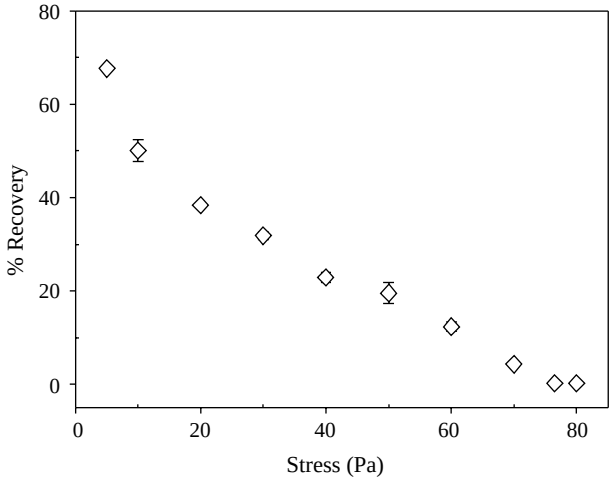

Fig. 5. The % recoverable strain as a function of the applied stress of 20 wt% highly doped PTAA suspension under field strength of 1 kV/mm.

field strengths, determined as [10]:

$$\%\ \text{recoverable strain} = \frac{(\gamma_i - \gamma_f)}{\gamma_i} \times 100 \quad (3)$$

where γ_i is the total strain acquired before removing the applied stress, and γ_f is determined from the average steady state strain. Consistent with the observations of Osubo and Ekamura [14], the % recovery decreases continuously with increasing applied stress and reaches zero at the yield point. As noted by Li et al. [15], at the yield point, the stress energy is completely dissipated by particle motion, as the particle fiber structure changes from one configuration to another. Thus, the ER fluid shows no elastic recovery at or above the critical stress [15].

Fig. 6 shows the compliance response of the 20 wt% HPT20 suspension at a constant stress of 50 Pa subjected to electric field strengths of 1, 2, and 3 kV/mm. At each field strength, the sample is in the nonlinear viscoelastic regime. In the creep phase, a decrease in the instantaneous creep compliance can be clearly observed with the increase of electric field strength. After removal of the applied stress, the recovery compliance increases with increasing electric field strength. Thus, the plastic strain response is decreased, and the elastic strain response increased, by increase in field strength. Moreover, it appears that, for this highly doped suspension, at fixed applied stress, with increasing field strength, there is an evolution from plastic solid to elastic solid behavior. Thus, at a field strength of 3 kV/mm, it appears that HPT20 has moved back into the linear viscoelastic regime, where it now behaves essentially as an elastic solid with $\gamma_C = \gamma_e = \gamma_R$. This presumably reflects an increase in the number of fully attached chains relative to unattached chains in the fibrillar aggregates at higher field strengths.

For HPT dispersions at a stress of 50 Pa, as evident in Fig. 4, it is possible to define an equilibrium creep compliance J_C as well as an equilibrium recovery compliance J_R. The electric field dependent values of J_C and J_R are shown in Figs. 7 and 8, respectively, for HPT samples of different concentrations.

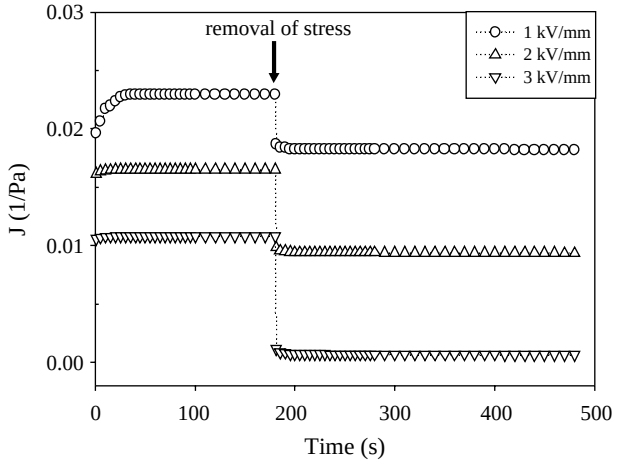

Fig. 6. Creep response of the 20 wt% highly doped PTAA suspension at a constant applied stress value of 50 Pa at various electric field strengths.

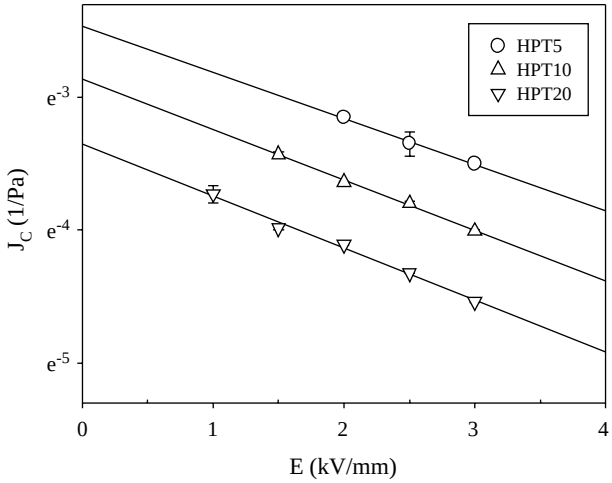

Fig. 7. Equilibrium creep compliance, J_C, of highly doped PTAA suspensions at a constant applied stress of 50 Pa at various electric field strengths.

It can be clearly seen that log J_C decreases linearly and log J_R increases linearly with the electric field strength. Qualitatively, these observations are consistent with the generally accepted mechanism for the ER effect in particulate dispersions [1,2]. Higher field strength induces a higher dipole moment, which increases the strength of the interparticle interactions, creating thicker and stronger fibrillar aggregates with more fully connected particle chains. These thicker fibers result in higher rigidity, and a more elastic response. From Figs. 7 and 8, it is further evident that J_C and J_R both decrease with particle concentration at a specified electric field strength, i.e. the values of J_C and J_R each decrease in the order HPT5 > HPT10 > HPT20. Increase of particle concentration increases the density and thickness of fibrillar aggregates. Evidently, this may increase both the elastic and plastic responses, i.e. both fully connected and unconnected chains are formed.

From Fig. 7, we may deduce that, at a specified particle concentration, the electric field dependence of J_C parameter

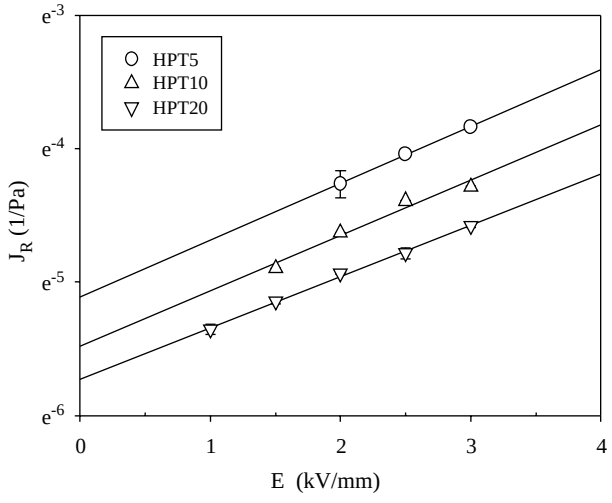

Fig. 8. Equilibrium recovery compliance, J_R, of highly doped PTAA suspensions at a constant applied stress of 50 Pa at various electric field strengths.

Table 2
Values of the fitting parameters J_{C0}, J_{R0}, E_C and E_R, describing the electric field dependence of the compliance of PTAA/silicone oil suspensions

ERFs	Creep phase		Recovery phase	
	ln J_{C0} (1/Pa)	E_C (kV/mm)	ln J_{R0} (1/Pa)	E_R (kV/mm)
HPT5	−2.46	2.87	−5.14	2.35
HPT10	−2.87	2.64	−5.48	2.41
HPT20	−3.36	2.56	−5.73	2.60
LPT20	−3.22	4.06	−5.83	1.86
UPT20	−2.63	3.95	−5.54	1.74

The parameters are determined from equations of $J_C = J_{C0}e^{-E/E_C}$ and $J_R = J_{R0}e^{-E/E_R}$.

can be written as

$$J_C = J_{C0}e^{-E/E_C} \quad (4)$$

where J_{C0} and E_C are fitting parameters. In principle, J_{C0} is the putative equilibrium creep compliance at zero electric field, which is an imaginary quantity, since, at zero field, no equilibrium compliance exists. E_C characterizes the sensitivity of the equilibrium compliance to an increase in field strength. The values of ln J_{C0} and E_C deduced from the fits in Fig. 7 are tabulated in Table 2. In the recovery phase, the electric field dependence of J_R parameter can be described by a similar relationship:

$$J_R = J_{R0}e^{E/E_R}, \quad (5)$$

where J_{R0} is the imaginary recovery compliance at zero field, and E_R is the corresponding field sensitivity parameter. From Fig. 8, the values of ln J_{R0} and E_R for the HPT5, HPT10, and HPT20 suspensions were determined and are tabulated in Table 2. It should be realized that the validity of Eqs. (4) and (5) are limited to electric field strength values between a lower bound, where a finite yield strength appears, and an upper bound where $J_C = J_R$, and a fully elastic response is observed. For the HPT20 sample, this upper bound is evidently reached at a field strength of 3 kV/mm (cf. Figs. 7 and 8).

A different perspective on the compliance response is obtained by considering the % recoverable strain, which is

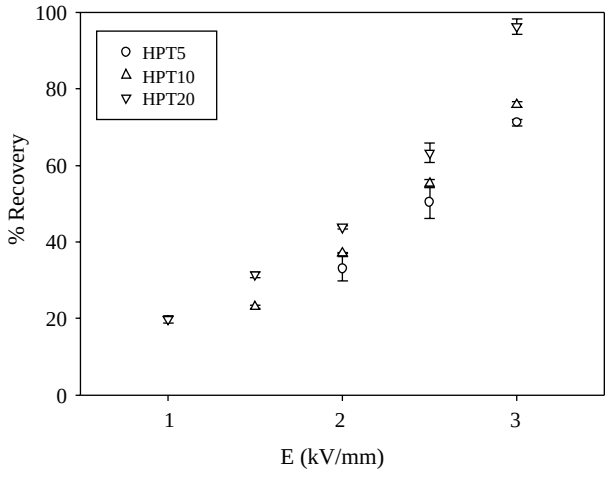

Fig. 9. The % recoverable strain as a function of the electric field strength for highly doped PTAA suspensions at a constant applied shear stress of 50 Pa.

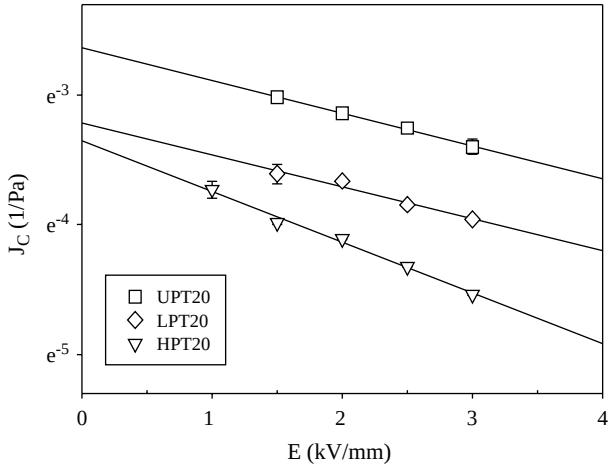

Fig. 10. Equilibrium creep compliance, J_C, of 20 wt% $HCLO_4$ doped PTAA suspensions at a constant applied stress of 50 Pa at various electric field strengths.

equivalent to the ratio $J_R/J_C \times 100$. These data are shown in Fig. 9, as a function of the electric field strength at various particle concentrations. As the electric field strength increases, the % recoverable strain increases strongly at a fixed applied stress, indicating an increase in elastic response relative to plastic response, as the electric field strength increases. Moreover, the % recoverable strain also increases with increasing particle concentration. This demonstrates that the overall result of an increase in field strength and particle concentration is an increase in elasticity of the suspension, i.e. there is a preponderance of fully connected versus unconnected particle strings in the fibrillar aggregates produced.

Figs. 10 and 11 show the effect of particle conductivity on the values of J_C and J_R for 20 wt% $HClO_4$ doped PTAA suspensions at various electric field strengths. At a specific electric field strength, the J_C and J_R parameters each decrease with increased particle conductivity, i.e. the values of J_C and J_R increase in the order HPT20 < LPT20 < UPT20. The J_C and J_R values also exhibit electric field dependences of the form

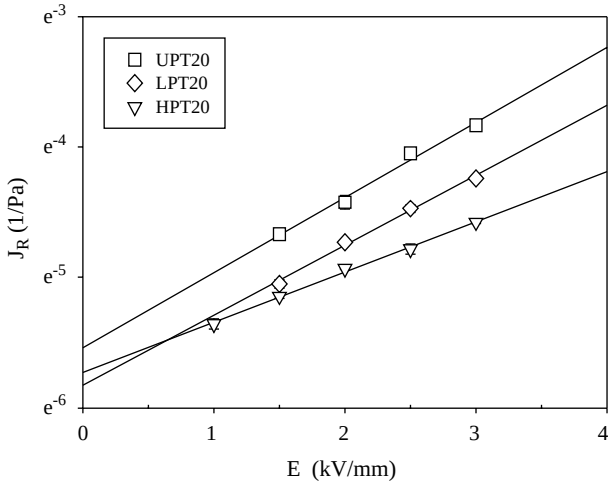

Fig. 11. Equilibrium recovery compliance, J_R, of 20 wt% $HCLO_4$ doped PTAA suspensions at a constant applied stress of 50 Pa at various electric field strengths.

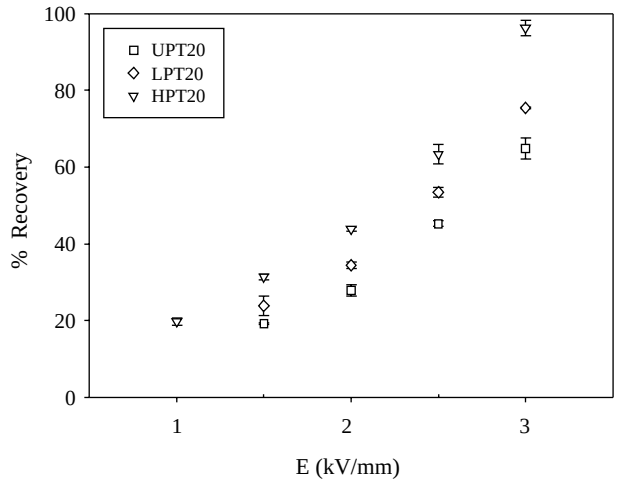

Fig. 12. The % recoverable strain as a function of the electric field strength for 20 wt%. $HCLO_4$ doped PTAA suspensions at a constant applied shear stress of 50 Pa.

$J_C = J_{C0}e^{-E/E_C}$ and $J_R = J_{R0}e^{E/E_R}$,, respectively. The values of ln J_{C0}, E_C, ln J_{R0} and E_R deduced from the fits in Figs. 10 and 11 are tabulated in Table 2.

From Table 2, it can be clearly seen that J_{C0} and J_{R0} decrease substantially with particle concentration and particle conductivity. Thus, an increase in particle conductivity has a similar effect to an increase in particle concentration, i.e. it results in an increase in the density and thickness of fibrillar aggregates at a specified concentration, which can cause an increase in both the elastic and plastic responses of the suspension. Moreover, it is evident from Figs. 10 and 11, and Table 2 that the electric field sensitivity parameters, E_C, and E_R, do not vary significantly with particle concentration, but do appear to depend on particle conductivity. Specifically, the E_C and E_R values of suspension HPT20, which has substantially higher conductivity than UPT20 and LPT20, are, respectively, significantly higher and significantly lower, than the corresponding values for LPT20 and UPT20. This is qualitatively consistent with expectation based on the electrostatic polarization model [20,21], which indicates that the net interparticle force is proportional to the square of the electric field, E^2, particle volume fraction, ϕ, and the relative particle polarizability β as $F \propto \phi K_f E^2 \beta^2$, where K_f is the dielectric permittivity of the continuous medium. Under DC or low frequency AC fields, the polarisability β is enhanced by an increased mismatch between the conductivities of the particles and the continuous medium [22]. Thus an increase in particle conductivity results in stronger interparticle interactions, and a more rapid decrease in equilibrium compliance with increase of field strength. Fig. 12 shows the effect of particle conductivity on the % recoverable strain of $HClO_4$-doped PTAA suspensions. The % recoverable strain increases substantially with particle conductivity at fixed electric field strength, indicating that the stronger interparticle forces result in an enhanced elastic response of the suspension, which evidently is magnified at higher field strengths (Fig. 12).

4. Conclusions

In this study, the creep response of poly(3-thiopheneacetic acid) particles doped with $HClO_4$ has been investigated. Consistent with literature reports for model ER systems, at a specified particle concentration and electric field strength, these PTAA suspensions exhibit an evolution with increase of applied stress from a linear viscoelastic response, with three components of instantaneous elastic strain, retarded elastic strain and viscous strain, to a nonlinear viscoelastic response, where the retarded elastic and viscous strains monotonically decrease and a plastic contribution to the instantaneous strain grows, followed by a viscoplastic solid behavior, with fully plastic instantaneous strain, and finally a transition from plastic solid to a plastic liquid at the yield stress. With increase in electric field strength at fixed particle concentration and applied stress, the viscoplastic response diminishes, and more elastic behavior ensues. For highly doped samples, at high-electric field strengths, a fully elastic solid response is observed in the linear viscoelastic regime. At fixed applied stress, the equilibrium compliance, J_C and steady state recoverable compliance J_R, were investigated as a function of electric field strength, particle concentration and particle conductivity. The results are found to be consistent with the anticipated effects of these parameters on the strength of interparticle interactions within the polarization model, and with the field-induced formation of thick fibrillar aggregates spanning the gap between the electrodes, each consisting of bundles of particle strings. Strings, which are fully connected to both electrodes generate an elastic response to the applied stress, whereas strings which are attached at only one end or are unattached generate a viscoplastic response. We observe that the % recoverable strain (equivalent to the ratio $J_R/J_C \times 100$) increases with increase of the electric field strength, particle concentration, and particle conductivity, indicating that the net effect of these changes in system parameters is an increase in elastic response, i.e. predominantly creation of fully connected particle strings.

Acknowledgements

The authors are grateful for the financial supports provided by The Thailand Research Fund (TRF): TRF-RGJ grant no. PHD/0128/2542; and TRF-BGJ grant no. BGJ/03/2544, the Petroleum and Petrochemical Consortium, and the Electroactive and Conductive Polymers Research Unit.

References

[1] Zukoski CF. Annu Rev Mater Sci 1993;23:45–78.
[2] Parthasarathy M, Kingenberg DJ. Mater Sci Eng 1996;R17:57–103.
[3] Voyles RM, Fedder G, Khosla PK. Proceedings of the IEEE international conference on robotics and automation; 1996.
[4] Kamath GM, Wereley N. Smart Mater Struct 1997;6:351–9.
[5] Pfeiffer C, Mavroidis C, Cohen YB, Dolgin B. Proceedings of the 1999 SPIE telemanipulator and telepresence technologies VI conference; 1999.
[6] Lee HJ, Chin BD, Yang SM, Park OO. J Colloid Interface Sci 1998;206:424–38.

[7] Kim SG, Kim JW, Choi HJ, Suh MS, Shin MJ, Jhon MS. Colloid Polym Sci 2000;278:894–8.
[8] Jang WH, Kim JW, Choi HJ, Jhon MS. Colloid Polym Sci 2001;279: 823–7.
[9] Jun JB, Lee CH, Kim JW, Suh KD. Colloid Polym Sci 2002;280:744–50.
[10] Cho MS, Lee JH, Choi HJ, Ahn KH, Lee SJ, Jeon D. J Mater Sci 2004;39: 1377–82.
[11] Kim YD, Park DH. Colloid Polym Sci 2002;280:828.
[12] Goodwin JW, Markham GM, Vincent B. J Phys Chem 1997;101:1961–7.
[13] Sim IS, Kim JW, Choi HJ. Chem Mater 2001;13:1243–7.
[14] Otsubo Y, Edamura K. J Rheol 1994;38:1721–33.
[15] Li WH, Du H, Chen G, Yeo SH. Mater Sci Eng A 2002;333:368–76.
[16] See H, Chen R, Keentok M. Colloid Polym Sci 2004;282:423–8.
[17] Lau KC, Shi L, Tam YW, Sheng P. Phys Rev E 2003;67 [Art. No. 052502].
[18] Chotpattananont D, Sirivat A, Jamieson AM. Colloid Polym Sci 2004; 282:357–65.
[19] Chotpattananont D, Sirivat A, Jamieson AM. Macromol Mater Eng 2004; 289:434–41.
[20] Klingenberg DJ, Swol FV, Zukoshi CF. J Chem Phys 1991;94:6160–9.
[21] Klingenberg DJ, Swol FV, Zukoshi CF. J Chem Phys 1991;94: 6170–8.
[22] Parthasarathy M, Klingenberg DJ. J Non-Newtonian Fluid Mech 1999;81: 83–104.
[23] Kim B, Chen L, Gong J, Osada Y. Macromolecules 1999;32: 3964–9.
[24] Chen L, Kim B, Nishino M, Gong J, Osada Y. Macromolecules 2000;33: 1232–6.
[25] Ferry JD. Viscoelastic properties of polymers. New York: Wiley; 1980 p. 42.